Limnology (2016) 17:273–289
DOI 10.1007/s10201-016-0481-z

RESEARCH PAPER

A multi-lake study of seasonal variation in lake surface evaporation using MODIS satellite-derived surface temperature

R. C. Phillips[1,2] · J. R. Saylor[3] · N. B. Kaye[4] · J. M. Gibert[5]

Received: 20 April 2015 / Accepted: 9 March 2016 / Published online: 16 April 2016

Abstract Knowledge of the evaporative loss from lakes and reservoirs is critical to water resources managers as well as to the overall understanding of the water balance in a given basin, geographical region, or continent. Existing methods for ascertaining evaporation from lakes and reservoirs include point measurements, water balance and mass transfer calculations, and proxy measurements using a pan. Point measurements using the eddy flux covariance method can be accurate, but are resource intensive and unsuited for determining spatial variation over a lake, or for obtaining measurements over many lakes. Mass balance methods cannot provide spatial variability and their accuracy depends on other portions of the water balance that can be challenging to obtain, such as leakage. Similarly, relatively recently deployed scintillation methods provide only an average for a strip across a lake and are also resource intensive and not suited for multi-lake studies. Evaporation pan measurements can also be used, though their accuracy is poor. Herein, we use a combination of Moderate Resolution Imaging Spectroradiometer (MODIS) satellite measurements of water surface temperature, measurements of wind speed, air temperature, and relative humidity from local NWS stations, and a mass transfer method, to demonstrate multi-lake evaporation measurements. Specifically, the seasonal variation in evaporation is obtained for the five major lakes in the Savannah River Basin (in South Carolina, USA): Lakes Jocassee, Keowee, Hartwell, Russell, and Thurmond. Since this approach requires only an existing satellite resource with global coverage and existing NWS stations, this method can potentially be ported to any lake where there is a nearby meteorology station. Hence, this method could be used by both water resource managers and limnologists alike. The possibility is discussed of extending this approach beyond a single basin to encompass an entire geographical region or continent.

Keywords Evaporation · Water resources · Modeling · Remote sensing

Handling Editor: Hidekatsu Yamazaki.

✉ J. R. Saylor
jsaylor@clemson.edu

[1] Wildlands Engineering, Inc, Charleston, SC, USA

[2] Department of Civil and Environmental Engineering, University of South Carolina, Columbia, SC, USA

[3] Department of Mechanical Engineering, Clemson University, Clemson, SC 29634, USA

[4] Department of Civil Engineering, Clemson University, Clemson, SC 29634, USA

[5] Department of Mechanical Engineering, Purdue University, West Lafayette, IN, USA

Introduction

Evaporation is a major component of the water balance of a lake, reservoir, or impoundment. This evaporative loss is of particular interest to water resources managers who require this information to effectively manage available resources (McJannet et al. 2013a). There are many methods for measuring surface evaporation from lakes and reservoirs, as reviewed below. However, each method has its own drawbacks, such as requiring significant on-site instrumentation, making only point (eddy co-variance) or line (scintillometry) measurements over a heterogeneous surface; not accurately representing the thermal behavior of the lake (pan measurements); or not accurately quantifying

the seasonal variation in evaporation (pan measurements). Accurate estimation of evaporation over shorter time scales (weeks or months) is becoming increasingly important as water resources become more stressed and short-term evaporation mitigation plans, such as the use of surfactant mono-layers (La Mer 1962; Barnes 1968; Bower and Saylor 2013; Saylor et al. 2000) are considered. In addition to its relevance to the quantity of available water, evaporation and other surface transport processes influence water quality and lake temperature.

Seasonal evaporation trends of open water bodies are often characterized by a bell curve with peak evaporation occurring during the summer months (Finch and Calver 2008; Penman 1948; Gupta 2001; Winter et al. 2003). However, many studies have shown shifts in seasonal evaporation, due to lake thermal inertia, causing peak evaporation to occur during fall and early winter months (Farnsworth et al. 1982; Liu et al. 2011; Rimmer et al. 2009). Additionally, inter-annual variability in lake evaporation has shown a large dependence on wind speed pulses and warm dry air fronts, as well as cold front activities (Liu et al. 2011; Blanken et al. 2000, 2003). Daily and seasonal variability in meteorological conditions over water bodies can in turn cause seasonal variations and shifts with respect to "typical" evaporation patterns. Consequently, a method for measuring evaporation that can provide higher temporal and spatial resolution in evaporation over a prolonged period of time may provide a more accurate estimate of lake evaporation.

Existing evaporation measurement methods

Perhaps due to its simplicity and convenience, one of the most commonly used evaporation measurement methods employed by water resource managers is pan evaporation measurements (Linsley et al. 1982; Yu and Brutsaert 1967; McJannet et al. 2013a) from registered National Weather Service (NWS) Class A evaporation pans. In this method, lake evaporation is obtained using a calculated pan coefficient, defined as the ratio of lake evaporation to pan evaporation (Brutsaert 1982; Gupta 2001),

$$K\mathrm{p} = \frac{E_L}{E_\mathrm{p}} \tag{1}$$

where K_p is the pan coefficient, E_L is the evaporation of a water body, such as a lake or reservoir, and E_p is the evaporation measurement from the pan.

There are a number of problems with using pan evaporation measurements. For example, pans have a thermal inertia that is significantly smaller than for even the smallest of ponds. As such, the time scale for thermal change in a pan is of the order of hours compared to months for many lakes. Evaporation pan measurements are often applied to lakes that are some distance away. For example, the pan evaporation measurements used by McJannet et al. (2013a) for comparison with other evaporation measurements were based on a pan that was 54 km from the impoundment tested. As a result of these problems, pan measurements often fail in several ways. Accordingly, it is quite problematic to use pan evaporation measurements for planning the use of short-term water resource conservation measures such as water use restrictions or evaporation suppression technologies (La Mer 1962; Barnes 1968; Bower and Saylor 2013; Saylor et al. 2000).

There are a number of other evaporation measurement methods that do not suffer from the inaccuracies of the pan method. These include water (Patra 2001) and energy (Momii and Ito 2008; Stannard and Rosenberry 1991) balance methods, scintillometry (McJannet et al. 2011, 2013a; McJannet et al. 2013b), eddy co-variance probes (Stannard and Rosenberry 1991), coupled mass, energy, and constituent balances (Assouline 1993), and the mass transfer method (or aerodynamic method) (Gupta 2001). These are each briefly described below.

A general expression for determining evaporation via the water balance method is (Patra 2001):

$$E = (P + I_\mathrm{sf} + I_\mathrm{gf}) - (O_\mathrm{sf} + O_\mathrm{gf}) + \Delta S \tag{2}$$

where E is in units of depth per unit time, P is the rate of precipitation over the lake surface, I_{sf} is the surface inflow per unit area, I_{gf} is the ground water inflow per unit area, O_{sf} is the surface water outflow per unit area, O_{gf} is the ground water outflow per unit area, and ΔS is the rate of change in storage per unit area. All the terms on the right-hand-side require on-site instrumentation to quantify. Furthermore, measurement of groundwater inflow/outflow is difficult and can result in significant uncertainties in E as obtained from Eq. (2) (Linsley et al. 1982).

An energy balance can be applied either at the lake surface, or for the entire lake water mass. The surface energy balance method (Henderson-Sellers 1986) is commonly expressed as (Brutsaert 1982):

$$E = \frac{R_n - H - G}{\rho h_\mathrm{w}} \tag{3}$$

where R_n is the specific flux of net incoming radiation, H is the specific flux of sensible heat into the atmosphere, and G is the specific flux of heat transferred into the lake all of which must be measured on site. The constant h_w is the latent heat of vaporization of water, and ρ is the density of water. This method has many measurement uncertainties, particularly with regard to G.

A full lake water heat balance is similar except that the net heat flux from the lake surface into the water body is

quantified in terms of a rate of change of heat content (Q_T) in the water (Stannard and Rosenberry 1991; Gianniou. and Antonopoulos 2007). That is:

$$E = \frac{1}{\rho h_w}\left(R_n - H - \frac{dQ_T}{dt}\right). \quad (4)$$

The thermal content of the water can be quantified by measuring the temperature profile in the lake using, for example, a vertical line of thermistors (Momii and Ito 2008; Verburg and Antenucci 2010).

The eddy co-variance method measures the vertical turbulent flux of water vapor at some distance above the lake. The measurement assumes that there is negligible horizontal gradient in the horizontal moisture flux below the probe. It may also be necessary to account for density effects (Webb et al. 1980), which would require additional meteorological data. This method effectively provides a point measurement of evaporation.

Recently, scintillometers have been used to measure the evaporation rate over lakes (McJannet et al. 2011, 2013a; McJannet. et al. 2013b; McGloin et al. 2014). A scintillometer measures the change in refractive index of air integrated over the length of a light or radio beam above the lake surface. This information, combined with meteorological data and a similarity model for the turbulent fluctuations of temperature and humidity, allows for calculation of the lake evaporation rate. The method is a line measurement across the lake, and, in a sense, falls between methods that obtain a single value for the entire lake, such as the energy balance methods, and point measurements, such as the eddy-flux method. As such, the method accounts for some of the spatial variability in lake conditions that have been observed in prior studies (Stannard and Rosenberry 1991).

Lake evaporation can also be measured using a mass transfer method, the approach used herein. In this method, evaporation is parameterized in terms of a mass transfer coefficient h_m. Specifically, the evaporation rate is quantified as:

$$E = \frac{h_m}{\rho}(q_s^* - q_a) \quad (5)$$

where q_s^* is the saturated specific humidity of water vapor at the temperature of the water surface, T_s; q_a is the specific humidity of water vapor at the ambient air temperature, T_a (the saturated specific humidity at T_a multiplied by the relative humidity, ϕ). The mass transfer coefficient h_m is typically parameterized in terms of the wind speed $\bar{u}$ (Brutsaert 1982; Sartori 2000; Gupta 2001; Penman 1948; Kohler and Parmele 1967; Adams et al. 1990). Hence, using Eq. (5) requires measurements of $(T_s, T_a, \bar{u}, \phi)$ typically requiring on-site instrumentation.

There have been multiple studies comparing the various measurement approaches described above. A study comparing eddy co-variance and energy balance measurements (Assouline and Mahrer 1993) found that the energy balance method resulted in lower estimates of evaporation than the eddy co-variance method early in the summer, but the results were similar later in the summer. They also observed times in which the evaporation estimates had opposite sign, with the energy method indicating net condensation compared to net evaporation measured from the eddy co-variance probe. A detailed study comparing scintillometry, pan, and surface energy balance methods was presented by McJannet et al. (2013a). Taking the scintillometer as their baseline, they found that, over the 18-month period of the study, the raw pan data gave very similar results to the baseline. However, once appropriate pan coefficients were used, this method underestimated the baseline evaporation. The surface energy method (Penman-Monteith) provided similar evaporation estimates to the baseline when all model terms were measured locally. However, the method overestimated the baseline when some terms were modeled or the weather data was collected over land. Of relevance to the present study is that discrepancy with the baseline found from using meteorologic data from a local weather station was similar to that of some model performance that used over-lake meteorologic data.

Applied appropriately, each of the measurement and estimation techniques described above can be used to estimate lake evaporation, with each approach having limitations due to cost, human resource requirements, temporal resolution, and spatial resolution. The cheapest approach discussed above, pan evaporation measurements, can provide reasonable estimates of annual evaporation (McJannet et al. 2013a). However, they have been shown to mis-characterize the seasonal variation in evaporation rate (Rimmer et al. 2009) due to the large difference in thermal inertia between the pan and the lake. Energy and mass balance methods suffer from an inability to provide any spatial resolution, have limited temporal resolution, and rely critically on the reliability of inflow and outflow measurements. The eddy-flux covariance method and the scintillometer methods provide greater temporal resolution, though at greater instrumentation and human resource costs, which limit the scale at which they can be used to, most commonly, a single lake. These approaches also typically rely on point measurements to characterize the entire lake. This fails to account for lake surface heterogeneity, as observed by Stannard and Rosenberry (1991). A final drawback of many of the approaches described is the lack of historical data for many lakes and reservoirs that could be used to establish long-term trends in evaporation

rate. The historical record of lake evaporation exists only for those lakes that have been chosen for study by scientists, or which have been documented by water resource managers. Historical data for a larger subset of the world's lakes would be useful in understanding historical year-to-year trends and variability in evaporation rates in order to better quantify the risk of water resource scarcity in the future.

An ideal method for estimating evaporation would be one that requires minimal or no instrumentation installation, provides some degree of spatial resolution over the lake surface, and can take advantage of historical data to provide past trends in evaporation. Herein, just such a method is presented where MODIS data is used to obtain spatially resolved lake surface temperature T_s and NWS meteorological stations are used to get $(\bar{u}, T_a, \phi)$, which are then used to obtain h_m from which E can be obtained from Eq. (5). Because MODIS provides spatially resolved T_s, spatial variation in E is obtained. Also, due to archiving of T_s and $(\bar{u}, T_a, \phi)$, evaporation trends extending into the past are possible. Herein, this approach is applied to the five major lakes of the Savannah River Basin using MODIS and NWS data that date back over a decade. Though applied only to five lakes, extension of the method to a much larger number of lakes and over a much larger geographical area requires only the processing of a greater amount of existing data. The overall goal of the paper is to demonstrate the feasibility of the approach, as well as to quantify the spatial and temporal variation in lake evaporation along the Savannah River basin.

Site description

The Savannah River Basin (SRB) originates in the Blue Ridge Mountains of Georgia, North Carolina, and South Carolina. The basin has a total drainage area of 27,400 km^2, of which 11,900 km^2 are in South Carolina, 15,100 km^2 are in Georgia, and 453 km^2 are in North Carolina (US-EPA, Region 4, SESD 1999). The basin serves as a major water source for more than 1.5 million people within Georgia, South Carolina, and North Carolina (U. S. Army Corps of Engineers 2013), as well as possessing a total power generating capacity of approximately 10,661 MW for residential and commercial use (HDR Engineering, Inc. of the Carolinas 2014).

A significant part of the upper Savannah River is controlled by the United States Army Corps of Engineers (USACE), which operates three multipurpose reservoirs: Lakes Hartwell, Russell, and Thurmond. Duke Energy constructed three additional reservoirs above Lake Hartwell as part of its Keowee-Toxaway project: Bad Creek Reservoir (a small pumped storage reservoir located above Lake Jocassee), Lake Jocassee, and Lake Keowee. Full pool elevations of Bad Creek, Jocassee, Keowee, Hartwell, Russell, and Thurmond are 704, 338, 244, 201, 145, and 101 m, respectively. A map of the basin and its main reservoirs is presented in Fig. 1. The volume of Bad Creek Reservoir and a few other small lakes are negligible, compared to the remaining five lakes in the SRB, and only those five lakes are considered in the remainder of this work. Geometric data for these five lakes are presented in Table 1.

Methods

The following is a description of the mass transfer methods used herein, as well as how pan evaporation data was collected to compare the mass transfer method results.

Mass transfer models

Three parameterizations for h_m were selected for use in applying Eq. (5) to obtain evaporation measurements. These three were chosen after organizing the numerous parameterizations into three general approaches: the turbulent boundary layer (TBL) approach, the general aerodynamic (AERO) approach, and the heat transfer (HT)

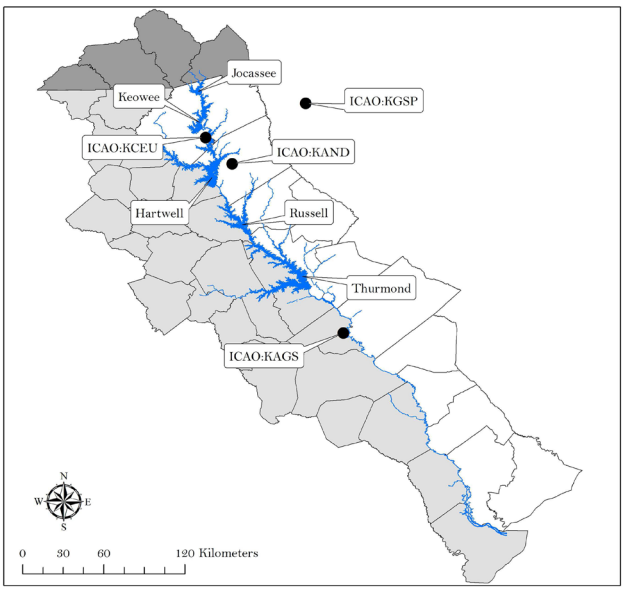

Fig. 1 Map of the Savannah River Basin, including major lakes, and nearby regional airport weather stations. North Carolina, South Carolina, and Georgia counties are represented as *dark grey, white*, and *light grey*, respectively. Data courtesy of the South Carolina Department of Natural Resources (SCDNR) and the United States Bureau of the Census (color figure online)

Table 1 Geometric information on the five major lakes in the Savannah River Basin

Lake	Surface area[a,c] (km^2)	Mean depth[b] (m)	Max depth[b] (m)	Shoreline length[c] (km)	Volume[a,c] (Mm^3)
Jocassee	30.6	48.1	99.4	121.0	1489
Keowee	75.0	16.0	90.5	482.8	1072
Hartwell	226.6	14.0	53.6	1548.2	3132
Russell	107.8	12.1	44.8	869.0	1262
Thurmond	283.3	11.3	43.3	1931.2	3072

[a] Calculated at full pool elevation

[b] Data supplied by South Carolina Department of Health and Environmental Control (SCDHEC)

[c] Data supplied by USACE

approach. All three are relationships for h_m as a function of wind speed. The TBL approach uses a parameterization for momentum transfer for a turbulent boundary layer, which is modified so that it can be applied to mass transfer. The AERO approach is a simplified version of the TBL method in which the mass transfer coefficient is a constant multiplied by the wind speed. Finally, the HT approach uses a parameterization for the heat transfer coefficient of a turbulent flat plate boundary layer, after which a heat-mass transfer analogy is used to develop a parameterization for h_m. One parameterization from each group was selected for investigation here, each of which has been used in past evaporation studies (Brutsaert 1975, 1982; Sartori 2000; Gupta 2001; McMillan 1971; Sweers 1976; Ham 1999; Penman 1948; Dalton 1802). These three parameterizations are:

$$h_m = \rho_a \bar{u} C_d^{1/2} / (13.6 Sc^{2/3} - 13.5 + C_d^{-1/2}) \quad TBL, \tag{6a}$$

$$h_m = \rho_a \bar{u} C_e \quad AERO, \tag{6b}$$

$$h_m = P_a C_1 (0.025 + 0.036 C_2 \bar{u}) / (0.622 h_w) \quad \text{HT}. \tag{6c}$$

Here, ρ_a is the density of air, $\bar{u}$ is the mean wind speed, C_d is the drag coefficient in the ambient air (and is a function of wind speed), C_e is the water vapor transfer coefficient, P_a is the atmospheric pressure, C_1 and C_2 are wind speed constants, h_w is the latent heat of vaporization of water, and Sc is the Schmidt number for water vapor in air:

$$Sc = \frac{\nu}{\mathcal{D}} \tag{7}$$

where ν is the kinematic viscosity of air, and $\mathcal{D}$ is the diffusion coefficient of water vapor in air. The main difference in each of these three approaches is the role of wind speed. For the TBL method, h_m is non-linear in wind speed, due to the wind speed dependence of C_d, while for the AERO method, h_m is linear in wind speed, and for the HT method, h_m is linear in wind speed with a constant zero offset. The terms TBL, AERO, and HT will be used hereinafter to refer to Eqs. (6a), (6b) and (6c), respectively.

Use of Eqs. (6a)–(6c) to estimate evaporation from a lake surface requires wind speed measurements taken at the same level as the remaining variables. Wind speed adjustments were made using power and logarithmic wind profiles typically associated with each of the aforementioned mass transfer equations (Brutsaert 1975, 1982; Sartori 2000; Gupta 2001; McMillan 1971; Sweers 1976).

To obtain evaporation using Eq. (5), measurements of $(T_s, T_a, \phi, \bar{u})$ are needed, and the means for doing this are now described.

$(T_a, \phi, \bar{u})$

The parameters T_a, ϕ, and $\bar{u}$ were all obtained from the Automated Surface Observing System (ASOS) (Nadolski 1998), which provides hourly values of (T_a, ϕ, and $\bar{u}$) from measurements taken at regional airports. Three regional airports within the SRB were selected to obtain (T_a, ϕ, and $\bar{u}$): Oconee Country Regional Airport (ICAO:KCEU); Anderson Regional Airport (ICAO:KAND); and Augusta Regional Airport (ICAO:KAGS). The locations of these airports are presented in Fig. 1. Proximity to the lake was used to determine which ASOS station to use for each lake. Hence, KCEU was used for Lakes Jocassee and Keowee, KAND was used for Lakes Hartwell and Russell, and KAGS was used for Lake Thurmond.

Satellite measurements of T_s

Water surface temperature T_s was obtained from the MODIS sensor on NASA's Terra and Aqua satellites. Daily MODIS land surface temperature (LST) level 3, 1-km nominal resolution data for Terra (MOD11A1, version 5) and Aqua (MYD11A1, version 5) were obtained from the NASA Earth Observing System Data and Information System (EOSDIS) from July 2002 to December 2012. The

Table 2 RMS error and bias from studies of lake-based and MODIS measurements of lake surface temperatures

Study	RMS error (K)	Bias (K)	Study location
Crosman and Horel (2009)	1.6		Great Salt Lake, UT, USA
Grim et al. (2013)	0.66	0.01	Great Salt Lake, UT, USA
Liu et al. (2015)	1.2–1.8		Lake Tahiu, China
Oesch et al. (2005)	1.25	−0.23	Lake Constance, Switzerland
Reinart and Reinhold (2008)	0.4	0.41	Lakes Vänern and Vättern, Sweden
Xiao et al. (2013)	1.46		Qinghai Lake, China

MOD11A1 and MYD11A1 LST products are generated from MODIS bands 31 (11 μm) and 32 (12 μm)(Wan 1999). The MODIS LST data is pre-processed to account for atmospheric and surface emissivity effects. Also, a cloud mask is incorporated for inland water estimates, providing a surface temperature measurement when there is a 66 % or greater confidence of clear-sky conditions (Wan 1999; Crosman and Horel 2009), otherwise no temperature is reported. It is noted that despite the name (Land Surface Temperature), the LST product is able to provide water surface temperature. Additionally, the LST from the Aqua and Terra platforms can be intercompared without correction (Wan et al. 2002, 2004; Wan 2008). Landsat 7-ETM imagery was used to develop a shoreline mask, which was used to exclude any MODIS LST pixels-containing land. The number of land-free pixels were 6, 1, 12, 3, and 19 for lakes Jocassee, Keowee, Hartwell, Russell, and Thurmond, respectively.

On-site measurements of T_s were not available for the lakes studied in this work, and so validation of the MODIS data used herein was not possible for the lakes studied. However, validation studies of MODIS T_s measurements of lake surfaces have been performed by several authors, as summarized in Table 2 which shows the RMS and bias errors between the MODIS measurement and in situ measurement for the lake studied, suggesting the reliability of this approach. The significance of these bias and RMS errors on the resulting evaporation measurements is further discussed in the final section of this paper. It is also noted that Schneider and Hook (2010) used ground validated satellite data from the Great Lakes to study lake surface temperature changes on a large number of uninstrumented lakes, an approach that is, effectively, identical to that used here.

Cloud contamination and miscellaneous satellite malfunctions resulted in gaps in T_s measurements. To illustrate this, the number of measurements obtained from Aqua and Terra are presented in Fig. 2 for Lake Hartwell for each of the 11 years analyzed in this work. Given a maximum of four satellite measurements per day for the Aqua/Terra combination, the overall data acquisition percentage was 54, 44, 61, 57, 66 %, for Lakes Jocassee, Keowee, Hartwell, Russell, and Thurmond, respectively. The relatively low data acquisition percentages present difficulty in developing a continuous daily evaporation time series to compare with pan measurements. To address this, a Fourier method was used to fill in the missing surface temperature measurements. Fourier analysis typically requires equally spaced data that was not available here, and so the Harmonic ANalysis of Time Series (HANTS) algorithm was used, which is often employed in the reconstruction of surface temperature data sets having such issues (Julien et al. 2006; Xu et al. 2013). The algorithm is a hybrid of a Fourier transform and a least squares curve fit.

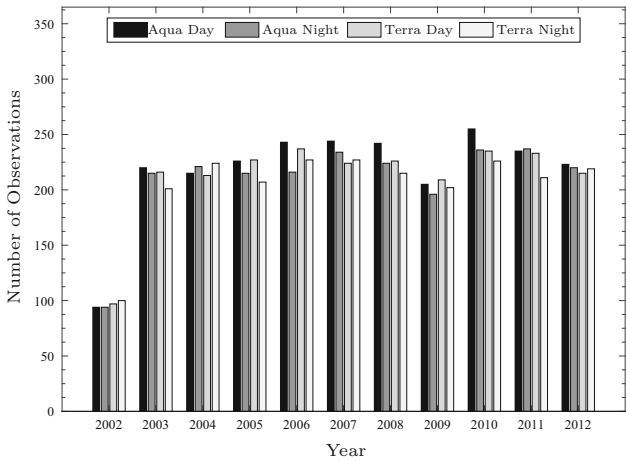

Fig. 2 Available surface temperature measurements for Lake Hartwell. Note that a maximum of 365 possible measurements are attainable for each of the Aqua and Terra day or night overpasses

The HANTS algorithm is controlled by five main parameters: (1) Number of frequencies (NOF), which describes how many terms to keep of the Fourier fit; (2) Hi/Lo/None suppression flag, which indicates whether high or low values, outliers, should be rejected during the curve fitting procedure; (3) Invalid data threshold range, which gives the range of valid data values; (4) Fit error tolerance (FET), which expresses the absolute difference in data values from the curve fit and the original data; and (5) Degree of overdeterminedness (DOD), which designates the minimum number of original data points for which the curve fit can be completed. NOF, FET, and DOD were the

most important parameters to estimate for controlling the output of the HANTS algorithm. The remaining parameters were relatively easy to determine. For this research, the suppression flag was set to none, while the invalid data threshold range was set to 0–100. This indicated that no outliers would be rejected during the curve fit between the range of 0–100 °C, which corresponds to the valid data range of the MODIS LST data.

A parametric study was conducted to estimate appropriate values for NOF, FET, and DOD. During this study, the HANTS algorithm was performed with variations of NOF, FET, and DOD for each of the MODIS LST data sets. Coefficients of determination were calculated using the HANTS and MODIS derived LST values to ensure an accurate fit. Visual inspection of each HANTS derived LST time series was also conducted. After performing the study and analyzing the HANTS derived LST data sets, appropriate values for NOF, FET, and DOD were selected. The parameter values selected for this work remained constant and did not vary by lake. NOF values selected for the HANTS Algorithm were 225, 200, 225, and 175 for Aqua day, Aqua night, Terra day, and Terra night satellite data sets, respectively. FET and DOD values selected for the HANTS algorithm were 5 and 6, respectively, for each satellite overpass. The calculated coefficient of determination for each lake MODIS LST data set is presented in Table 3. The average coefficient of determination between the reconstructed time series and the data was 0.94. A sample HANTS time series is plotted in Fig. 3 along with the original MODIS LST data for Lake Hartwell's Aqua daytime overpass.

The Terra and Aqua satellites have a sun-synchronous, near-polar, circular orbit, with a revisit time of approximately 12 h and a 1-km nominal spatial resolution (0.928 km actual at Nadir). The Terra satellite has a local equatorial crossing time of approximately 10:30 A.M. and 10:30 P.M. in a descending and ascending mode, respectively, while the Aqua satellite has a local equatorial crossing time of approximately 1:30 A.M. and 1:30 P.M. in a descending and ascending mode, respectively. The above overpass times are nominal, and fluctuations do exist. Overpass times for Terra and Aqua are presented in Fig. 4 over Lake Hartwell for the entire period of the present study.

Table 3 Coefficients of determination for HANTS algorithm fit of MODIS LST data

Lake	Aqua day	Aqua night	Terra day	Terra night
Jocassee	0.94	0.92	0.93	0.92
Keowee	0.93	0.95	0.94	0.92
Hartwell	0.95	0.94	0.95	0.94
Russell	0.94	0.94	0.94	0.94
Thurmond	0.95	0.93	0.94	0.94

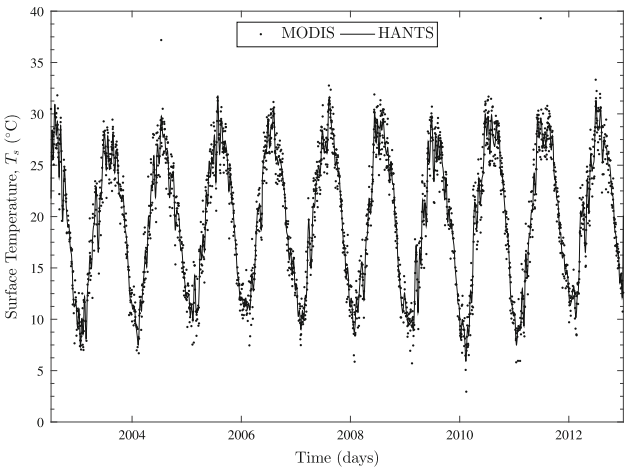

Fig. 3 Lake Hartwell MODIS data and HANTS time trace for T_s for the Aqua daytime overpass

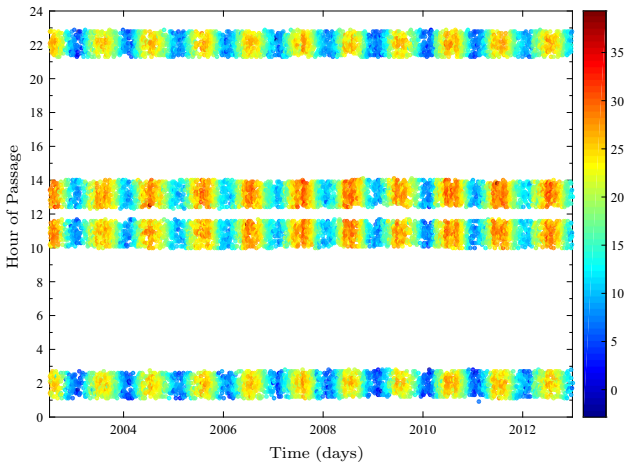

Fig. 4 Data acquisition times for T_s measurements obtained from Terra and Aqua satellites over Lake Hartwell. Values for the spatially averaged T_s are indicated by *color*. Temperatures in color palette are in °C (color figure online)

The value of T_s is also presented for each overpass, indicated in color. Since the max-min variation in overpass times was about two hours, and since measurements of $(T_a, \phi, \bar{u})$ are reported by ASOS on only an hourly basis, the nominal overpass times of 11 A.M., 1 P.M., 10 P.M., and 2 A.M. were used for T_s measurements. Hence, evaporation measurements using the mass transfer method were obtained using T_s values from the spatially averaged LST data and the corresponding hourly T_a, ϕ, and $\bar{u}$ measurements from the ASOS station closest to the corresponding lake. The evaporation rates obtained by the TBL, AERO, and HT methods were computed by scaling the hourly net evaporative flux by the water density calculated at T_s so that all methods report evaporation in units of length per unit time. Finally, the four hourly evaporation

rates obtained from each method were averaged to give a daily estimate of reservoir evaporation.

There was some amount of missing ASOS data. However, no steps were taken to fill in values for (T_a, ϕ, $\bar{u}$). Instead, the resulting gap in the evaporation rate time traces was filled using an elliptical interpolation function, allowing for a continuous daily evaporation rate time series for each lake from July 2002 to December 2012.

Pan measurements

Pan evaporation measurements were compiled to compare with the results of the mass transfer method described above. Measured pan evaporation values must be multiplied by a calculated pan coefficient, Kp, to appropriately estimate lake evaporation via the pan method [see Eq. (1)]. Pan coefficients for registered Class A pan evaporation observations have been developed by government agencies, researchers, and engineers. While it is understood that a pan coefficient of 0.70 is a good overall standard estimate (Finch and Calver 2008; Farnsworth et al. 1982; Boyd 1985), it has been found that pan coefficients can experience strong monthly variations (Finch and Calver 2008; Farnsworth et al. 1982; Boyd 1985). Consequently, a set of monthly pan coefficients was developed for use with the pan method. Furthermore, due to geographical and geometric differences between each or the major SRB lakes, it was assumed that each lake would need its own set of unique monthly pan coefficients. This approach is consistent with current modeling practice by the USACE along the SRB.

Several sets of pan evaporation measurements are available throughout the Savannah River Basin. However, pan data from the Class A pan located in Clemson, SC is the only available data set with measurements dating back to the development of the FWS grids (1956–1970), as well as covering the period of record for this study. As a result, these daily pan evaporation data measured in Clemson, SC were used. These were obtained from National Oceanic and Atmospheric Administration (NOAA)'s National Climatic Data Center (NCDC).

A monthly pan coefficient was developed for each of the lakes within the basin through the use of the FWS evaporation estimates from NOAA's digitized evaporation maps (Farnsworth et al. 1982) and the pan measurements obtained from the Clemson Class A pan. Monthly averages of daily FWS evaporation for each lake were calculated from the NOAA map ($\mathrm{FWS_{grid}(month)}$). These were combined with monthly averages of the daily evaporation rate measured by the Clemson, SC pan ($E_{\mathrm{pan}}(\mathrm{month})$), using the same period of record to calculate monthly pan coefficients for each lake using the equation:

$$K_{\mathrm{p}}(\mathrm{month}) = \frac{\mathrm{FWS_{grid}(month)}}{E_{\mathrm{pan}}(\mathrm{month})}. \quad (8)$$

Application of Eq. (8) gave a set of monthly pan coefficients to describe evaporation from each of the major SRB lakes using Clemson Class A pan observations. The monthly pan coefficients are presented in Fig. 5a. The corresponding daily pan evaporation rate is calculated by multiplying the evaporation rate measured by the pan on a particular day ($E_{\mathrm{pan}}(\mathrm{day})$) by the appropriate monthly pan coefficient. That is,

$$\mathrm{Evaporation(day)} = K_{\mathrm{p}}(\mathrm{month})\mathrm{Evaporation_{pan}(day)}. \quad (9)$$

The daily pan data was converted into lake evaporation rates for each lake using Eq. (9) and the coefficients shown in Fig. 5a. Hereinafter, when referring to pan measurements, it is the left-hand side of Eq. (9) that is being referred to.

The monthly average of the daily evaporation rates for each SRB lake corresponding to the Clemson Class A pan Period of Record (POR) are shown in Fig. 5b. Figure 5a shows a large seasonal variation in K_{p}. However, the overall average lake evaporation from each of the major SRB lakes were approximately equal with little variation in magnitude, which is a major downfall of using Class A pan measurements to estimate lake evaporation. Since the pan does not take into account the thermal behavior of the lake, regional variations of lake evaporation are harder to identify.

A daily evaporation rate time series was developed for each of the major SRB lakes using the monthly derived pan coefficients and the Clemson pan data. Some gaps occurred in the daily lake evaporation estimates, due to missing observations in the Clemson Class A pan, and these were filled using a linear interpolation function.

Results

Results are presented for the temporal variation in evaporation on both annual and monthly time scales and for the spatial variation in evaporation across the lake surface.

Yearly evaporation rates

Continuous daily time series of evaporation for each of the five major lakes in the SRB were calculated using the three mass transfer methods described in the previous section, and compared to pan evaporation measurements. Daily pan evaporation was calculated using daily data from the

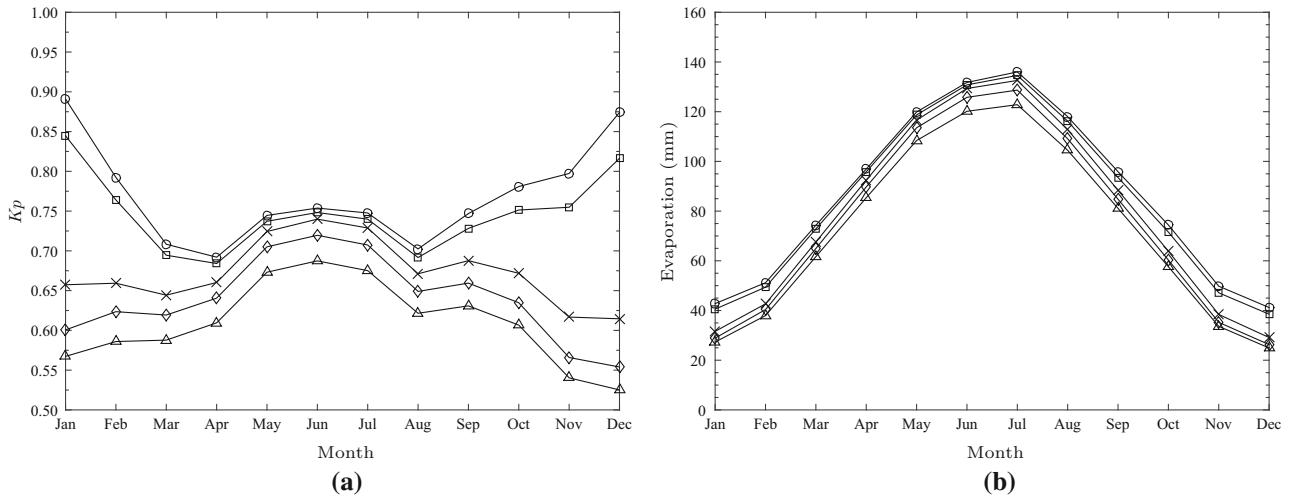

Fig. 5 **a** Monthly derived pan coefficients, K_p; **b** average monthly lake evaporation corresponding to Clemson Class A POR: Jocassee (*triangle*); Keowee (*diamond*); Hartwell (*cross*); Russell (*square*); and Thurmond (*circle*)

Clemson pan and the monthly pan coefficients shown in Fig. 5a. The ASOS and MODIS data were used to calculate the daily TBL, AERO, and HT [Eqs. (6a)–(6c)] evaporation totals. All four daily time series spanned the same POR, namely July 2002 to December 2012. The daily time series were used to calculate the annual total evaporation for each lake and each method. These are plotted in Fig. 6 and show a broadly similar annual variation in evaporation for each of the four evaporation data sets across all five lakes. With the exception of Lake Thurmond, the pan evaporation data shows the same qualitative year-to-year trends, as do the mass transfer data sets. The pan data does, however, exhibit less year-to-year variability than the mass transfer data. The coefficient of variation (COV) for the pan data was approximately 0.07 for each lake, while the COV for the mass transfer methods ranged from 0.2 to 0.22. Averaged over the period of record, the annual total pan evaporation falls within the range of values seen in the mass transfer data except for Lakes Jocassee and Thurmond. This is shown in Fig. 7.

The yearly percentage difference between the mass transfer methods (TBL, AERO, and HT) and the pan data was calculated and averaged, for each lake. The data is summarized in Table 4, along with the average for each lake and each method. In general the pan measurement showed higher levels of evaporation than the mass transfer methods; ten of the 15 average percent differences were negative. However, this data is slightly skewed by the AERO method, which gave lower evaporation totals than the pan for all five lakes.

The average percentage difference of all the methods ranged from +16 % for Lake Keowee to −31 % for Lake Thurmond. On average, the mass transfer methods reported lower annual average evaporation compared to the pan data. The only exception to this was Lake Keowee, for which the mass transfer methods predicted 16 % higher annual average evaporation. The satellite measurements of surface temperature for Lake Keowee were noticeably higher than for the other lakes, despite being at a slightly higher elevation than all but one of the lakes measured. This is likely, because the only MODIS pixel that was pure lake water was located north of the Oconee Nuclear Station, as can be seen in Fig. 8.

Water resources managers seeking to use the approach presented herein, but wanting to have results that provide similar yearly average totals to historical pan measurements, should use the historical MODIS and ASOS data to establish which mass transfer method best matches their pan data. For the SRB, this would be either the TBL or HT methods (see Table 4). Given the absence of absolute ground truth and the known issues with pan measurements, such a comparison should not be taken to indicate which mass transfer method is the best in an absolute sense.

Monthly evaporation rates

One goal of this study was to investigate the seasonal variation in lake evaporation in the SRB using two different methods for measuring evaporation. The four daily time series (three for the mass transfer method and one for the pan measurements) were used to calculate four monthly averaged evaporation totals for each lake; these are presented in Fig. 9. The data clearly show a significantly different seasonal behavior between the pan data and the mass transfer methods. For all five lakes, the pan data

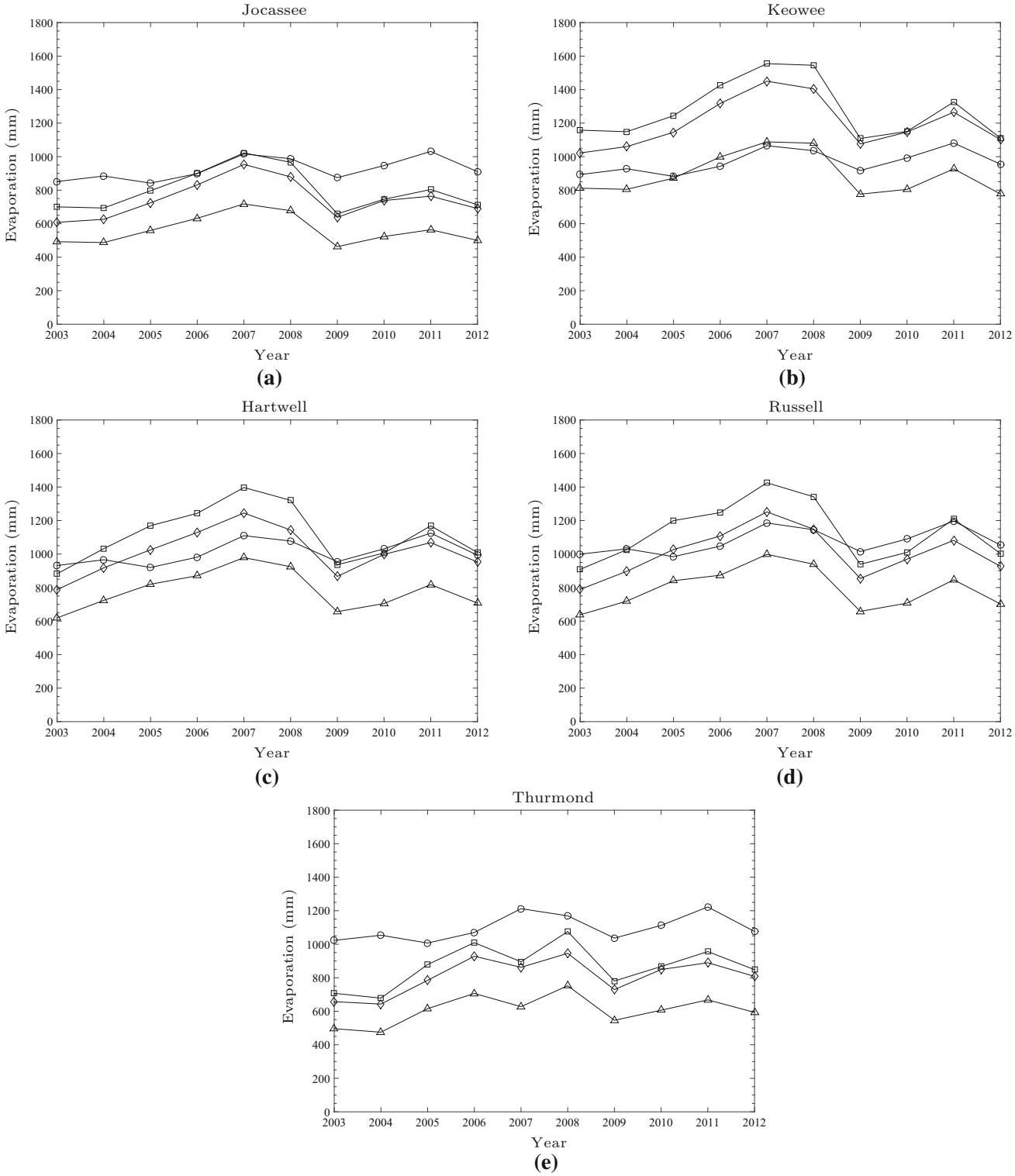

Fig. 6 Yearly lake evaporation corresponding to MODIS period of record for TBL (*square*), AERO (*triangle*), HT (*diamond*), and Pan (*circle*): **a** Jocassee; **b** Keowee; **c** Hartwell; **d** Russell; and **e** Thurmond

shows a peak in early to mid summer, while the mass transfer methods show a range of seasonal behaviors, none having a peak in the summer. Most of the lakes show two peaks in evaporation, one in the spring and one in the fall. The exception is Hartwell, which exhibits a single peak in the fall.

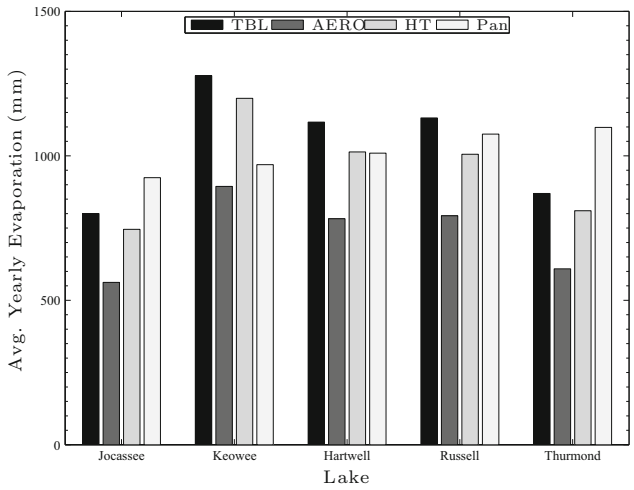

Fig. 7 Long-term yearly average lake evaporation

Table 4 Average percentage difference in annual evaporation from the pan data for each of the three mass transfer methods

	TBL (%)	AERO (%)	HT (%)	Mean (%)
Jocassee	−14	−39	−19	−24
Keowee	32	−7.8	24	16
Hartwell	11	−23	0.3	−3.9
Russell	5.0	−26	−6.7	−9.4
Thurmond	−21	−45	−26	−31
Mean	2.5	−28	5.8	

Spatial variability in lake surface evaporation

One benefit of the method described in this paper is that, for large enough lakes, the MODIS data can be used to obtain spatially resolved measurements of E for a lake. This can be used to investigate spatial variations in evaporation, and of course, the measurements can be averaged to provide the surface averaged value of E. Spatial variations in T_s obtained from MODIS can be significant, as shown in Fig. 10, which shows the mean lake to ambient air temperature difference plotted against the standard deviation in the spatial distribution of temperature over the surface of Lake Hartwell. Plots are shown for each satellite overpass time, and show that there are regularly spatial variations in lake surface temperature of up to 2K. For the period of record, over one-fifth of the satellite overpasses recorded a spatial standard deviation (σ_{TL}) in lake surface temperature that is greater than 50 % of the mean lake to ambient temperature difference (δT), indicating that there will be significant spatial variation in T_s, which will lead to similar spatial variations in E. The spatial variation in surface temperature on each lake in the SRB is illustrated in Fig. 8.

The magnitude of the spatial variation in evaporation is significant. Figure 11 shows histograms of the spatial COV of evaporation on Lake Hartwell calculated using the AERO method [Eq. (6b)]. Histograms are shown for each overpass time. The greatest spatial variation is observed during the night time overpasses; in particular, the early morning AQUA overpass. The average Lake Hartwell spatial COV for each overpass time and each mass transfer method [Eqs. (6a)–(6c)] are shown in Table 5. In all cases, the COV is lower for the daytime overpasses, though for all overpasses, the average COV is greater than 0.3. This indicates substantial spatial variation and suggests that point measurements of evaporation using, for example, an eddy covariance probe, could result in errors in lake evaporation measurements.

An area average is required to calculate the lake evaporation. Either the lake surface temperature can be averaged and then Eqs. (5) and (6a)–(6c) used, or the evaporation rate for each location can be calculated and then averaged. As the evaporation rate is only a weakly non-linear function of the temperature difference the averaging order makes little difference. This is illustrated in Fig. 12, which shows scatter plots of the spatially averaged lake evaporation rate, $E(X)$, versus the lake evaporation rate calculated using the spatially averaged surface temperature, $E(T)$, for two mass transfer methods applied to Lake Hartwell.

Discussion and conclusions

Three mass transfer methods were used for estimating lake evaporation along the SRB using remotely sensed lake surface temperature measurements. Daily, monthly, and yearly evaporation from the major lakes in the SRB were then obtained. Mass transfer based evaporation rates were compared with pan evaporation rates. In general, the yearly evaporation rates calculated using the mass transfer methods were lower than the pan measurements.

The percent difference between the mass transfer methods and the pan data averaged over the POR ranged from +16 to −31 %. However, for a specific year, they ranged from 51 % (2006 TBL on Lake Keowee) to −55 % (2004, AERO on lake Thurmond). These numbers are similar in magnitude to previous studies that compared pan data to other methods. For example, McJannet et al. (2013a) found that the percent difference between their pan data and a number of other measurements (eddy co-variance, scintillometer, and Penman) ranged from 25 to 61 %, with the pan measurements being lower than those for all the other methods. It should, however, be noted that the period of record for McJannet et al. (2013a) was 18 months

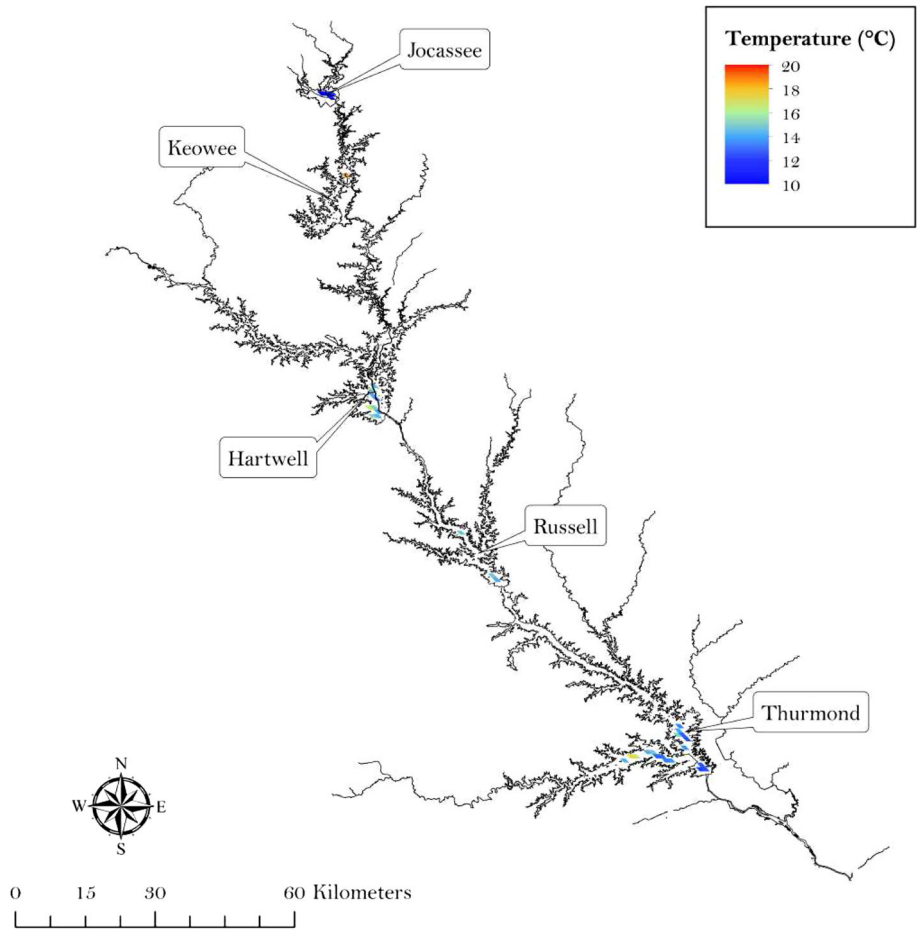

Fig. 8 Map of the Savannah River Basin, showing sample pixel temperatures for each of the major lakes. The figure is based on the MODIS sensor from the AQUA daytime overflight for 5 May 2005 (color figure online)

compared to 10 years for the present study; combined together, the statistical significance of these observations is increased.

From the daily lake evaporation rates, long-term monthly average evaporation rates were developed and presented. Mass transfer methods showed similar trends, although different magnitudes. The seasonal trend of the mass transfer methods each differed significantly from the pan trend. The mass transfer data generally produced lower rates of lake evaporation during the summer and higher rates of fall and winter evaporation, when compared to the pan data. This is likely due to the air temperature and humidity dropping more rapidly in the fall than the lake temperature. As the lake cools in the fall, there is significant sensible and latent heat release into the atmosphere prior to lake overturning.

The measured peak evaporation rate in the fall is consistent with the long-term evaporation rate from Lake Kinneret in Israel (Rimmer et al. 2009), which has very similar average daily temperatures to the SRB throughout the year, though Lake Kinneret is located in a dryer climate compared to the SRB. Lake Kinnert is also similar in scale to lake Hartwell; its volume is 33 % larger than Hartwell, the largest lake on the SRB. However, the lake is much less sinuous and has a surface area that is 27 % smaller than Lake Hartwell, such that the average depth of Kinneret is 60 % greater than Hartwell's. The maximum depth in Hartwell is 16 % greater than Kinneret.

The method proposed has many significant advantages over current approaches to measuring lake evaporation rate. Firstly, the approach requires no additional instrumentation, provided there is a near-by meteorological station from which to get wind speed, air temperature, and humidity. If this meteorological station is part of the ASOS system, then all of the required data can be downloaded from online data repositories; $(\bar{u}, T_a, \phi)$ from ASOS and T_s from EOSDIS. As such, evaporation estimates can be made using a computer with an internet connection. This is particularly important for larger multi-use lakes, such as many of those on the SRB. Secondly, the lake surface temperature measurements used are averages of multiple measurements over the lake surface, rather than being single point measurements. This is a potentially significant improvement, as analysis of the spatial variability of lake surface temperatures over SRB lakes

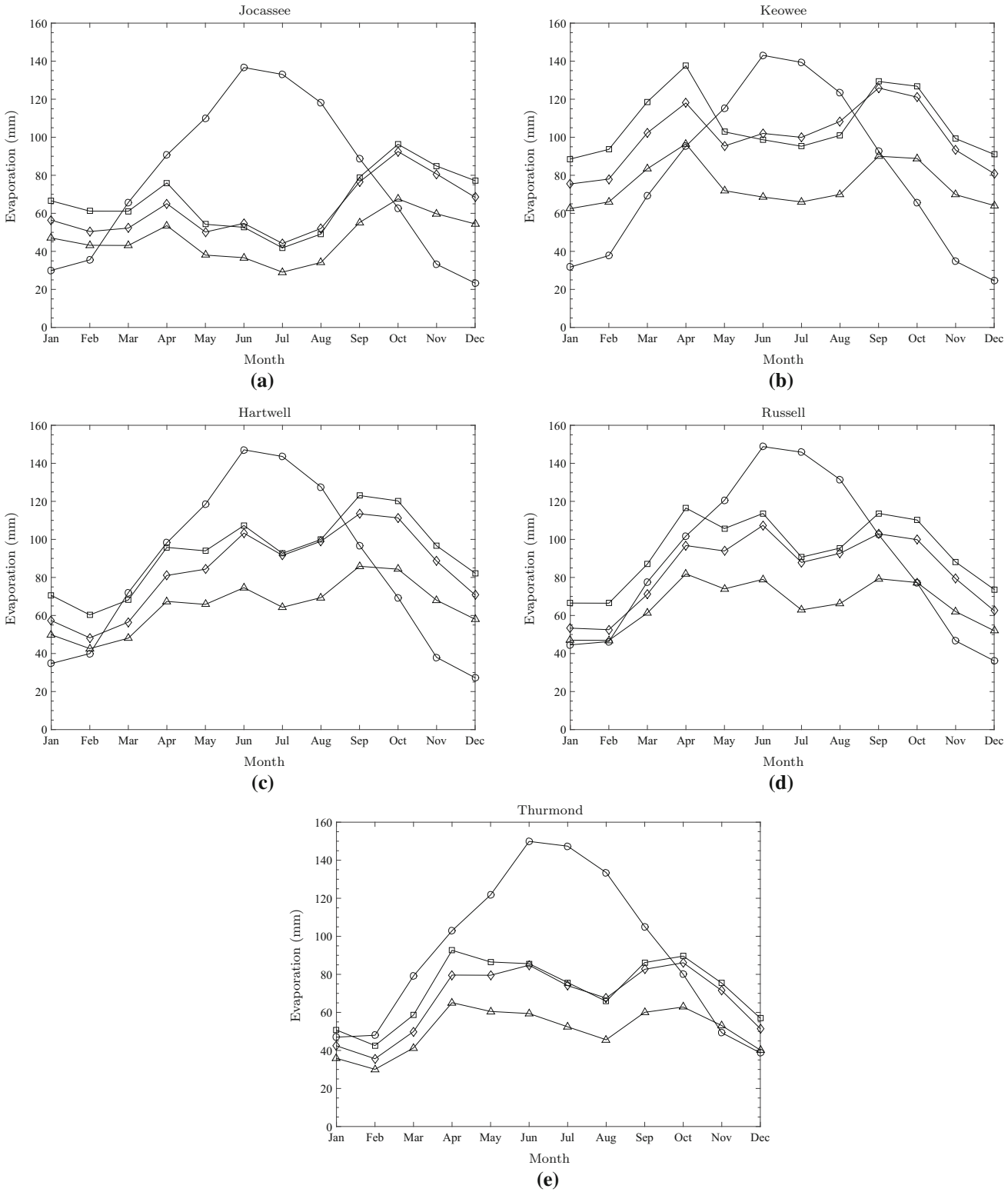

Fig. 9 Monthly average lake evaporation corresponding to MODIS period of record for TBL (*square*), AERO (*triangle*), HT (*diamond*), & Pan (*circle*): **a** Jocassee; **b** Keowee; **c** Hartwell; **d** Russell; and **e** Thurmond

showed that the standard deviation in spatial temperature was typically 20–30 % of the lake surface-to-air temperature difference. The number of MODIS pixels used to obtain T_s in the present study was admittedly small (and for Lake Keowee, only one land-free pixel was available). However, there are obviously many lakes of much larger extent for which

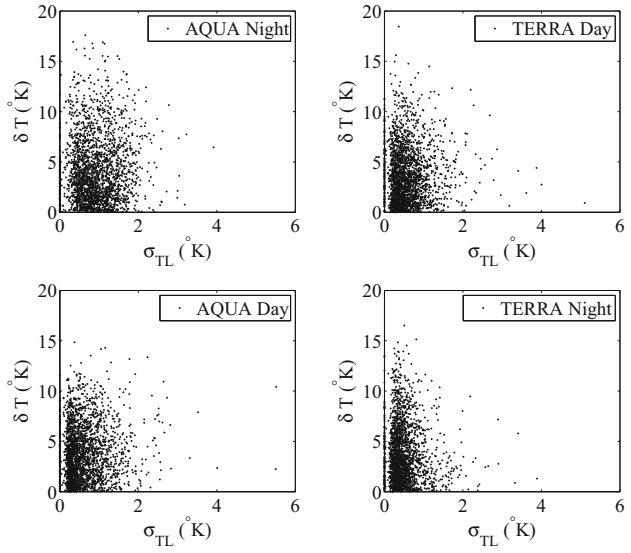

Fig. 10 Scatter plot of the temperature difference between the ambient and lake spatially averaged surface temperature (δT) versus the spatial standard deviation in the lake surface temperature (σ_{TL}) for each satellite overpass time for lake Hartwell

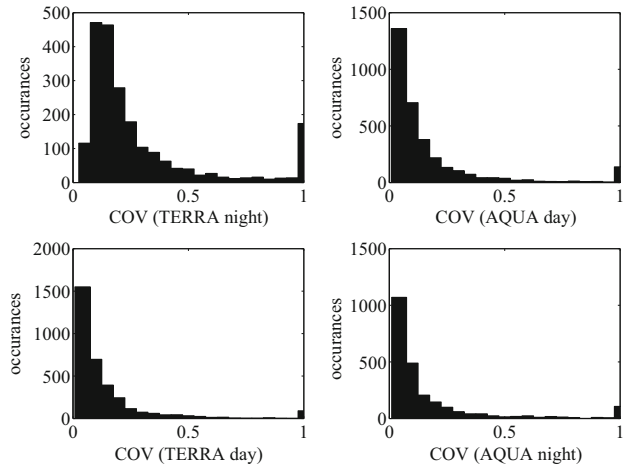

Fig. 11 Histograms for each overpass time of the coefficient of variation in the spatial distribution of lake surface evaporation for Lake Hartwell using the AERO method (all COV values greater than one are shown as a *single bar* at COV = 1)

Table 5 Average evaporation spatial coefficient of variation for Lake Hartwell

	AQUA night	TERRA day	AQUA day	TERRA night
AERO	0.50	0.31	0.33	0.40
TBL	0.50	0.31	0.35	0.41
HT	0.59	0.31	0.39	0.56

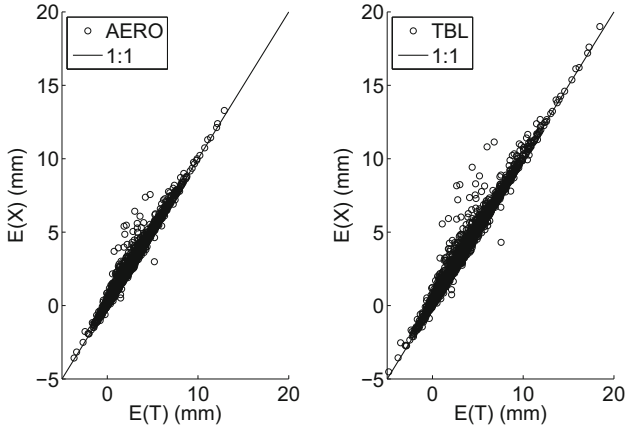

Fig. 12 Scatter plot of the spatially averaged lake evaporation rate, $E(X)$, versus the lake evaporation rate calculated using the spatially averaged surface temperature, $E(T)$ for the AERO method (*left*) and TBL method (*right*). The *solid line* represents exact agreement

this method would provide an even greater advantage over current single point approaches to evaporation measurement.

The present study used the MODIS sensors on the AQUA and TERRA satellites, though other satellite-based measurements are available. Table 6 presents a list of current satellite-based sensors. All the satellites listed make two measurements per day, and, with the exception of the Suomi NPP satellite, have a spatial resolution of approximately 1 km. Improved spatial resolution could be gained through the use of the Suomi NPP measurements (0.75 km resolution), though this gain is offset by significantly reduced thermal resolution and a much shorter period of record. A detailed land-based study would be required to establish the minimum spatial resolution required to fully quantify the spatial variability of lake surface evaporation. An additional benefit of using a higher spatial resolution would be an increase in the number of water-only pixels available for each lake. This is particularly true for smaller lakes, or long narrow lakes with multiple small inlets, such as those on the SRB (see Fig. 8).

The method described herein enables long-term studies of lake evaporation to be conducted, as the repository of lake surface temperatures from the MODIS sensors dates back to June 2002. Further, given the global coverage of the Terra and Aqua satellites, the method described could be used to do basin, regional, and ultimately global scale analysis of historical evaporation trends that could be used as part of a water availability risk analysis. Of especial use to limnologists, this method could be used to develop statistics of evaporation over numerous lakes. Water resources managers can also use this approach for shorter evaporation calculations. Because the method described results in a physically realistic seasonal trend in

Table 6 Available satellite-based surface temperature measurements

Satellite	Sensor	Spatial resolution (km)	Temporal resolution (h)	Thermal resolution (K)	Period of record
AQUA	MODIS	1	12	1	1999-present
TERRA	MODIS	1	12	1	2002-present
Suomi NPP	VIIRS	0.75	12	2.4	2011-present
NOAA	AVHRR	1.1	12	1.6–2.3	1978-present

evaporation, it could be used for short-term water availability calculations during droughts. This method, therefore, is of important utility to both limnological scientists and water resource managers.

One drawback of this work is that ground truth measurements for lake surface temperature were not available for the present study. However, there are numerous published studies that have compared MODIS measurements of lake surface temperatures with on-lake measurements. These studies report both the RMS error between the land and satellite measurements, as well as the bias. The results of these studies are summarized in Table 2 and show that the average RMS error reported is 1.2K with an average bias of 0.1–0.2K. The bias values reported are very small compared to typical air-to-lake surface temperature differences, and, as such, will only introduce significant error in the evaporation measurement on days with very small temperature differences, and, therefore, low evaporation rates. Moreover, low evaporation days, while common, do not contribute significantly to long-term evaporation totals. This is illustrated in Fig. 13, which shows a normalized histogram of the daily evaporation totals, calculated for Lake Hartwell using the AERO method, with the cumulative distribution function for the total evaporation over the period of record. While half the days over the period of record had less than 2 mm of daily evaporation, they only contributed about one-quarter of the total evaporation. As such, any small bias error will not significantly influence evaporation totals over longer periods of, say, a month or greater.

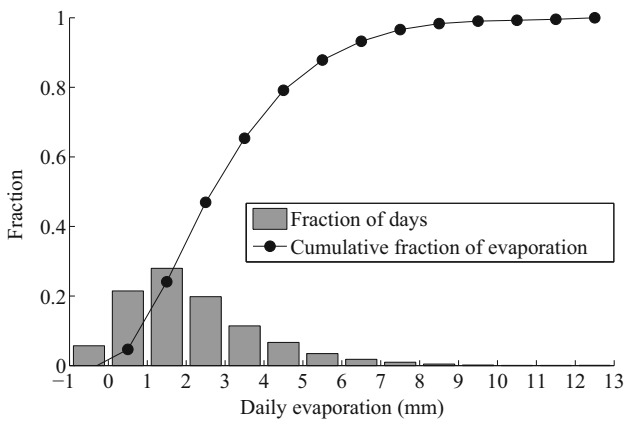

Fig. 13 Normalized histogram of the distribution of daily evaporation totals (based on the entire period of record) for Lake Hartwell using the AERO method (*bars*) and the cumulative distribution function for the total evaporation over the period of record

The RMS errors reported in the literature are significantly larger than the bias errors and may, therefore, have a greater impact on individual evaporation measurements. However, as the evaporation rate is only a weakly nonlinear function of the lake surface to ambient air temperature difference (see Fig. 12), random errors in individual measurements will average out to only a small systematic error over time. A standard error analysis was conducted for the mass transfer models that incorporated the measurement uncertainty in wind speed, air temperature, relative humidity, and MODIS RMS error. This estimated uncertainty for an individual measurement was 71 %. Averaged over the approximately 1200 measurements for each month over the 10-year period of record results in an uncertainty in the monthly average of approximately 2 %. This error analysis will likely overestimate the uncertainty, as the percentage uncertainty will be lower on high evaporation rate days, which contribute the most to monthly and yearly evaporation totals (see Fig. 13).

As noted earlier, the pixel size is nominally 1 km on a side. As a result, a statistical analysis of lakes would necessarily exclude any lakes smaller than this size. This would also rule out larger lakes that are highly sinuous. The method also requires that there is a meteorological station close to the lake. This is usually the case in densely populated areas, though more remote lakes may not meet this criteria. The use of meteorological station data that is not on the lake or on the lake shore also introduces some error into the calculations. This error is difficult to quantify. However, as a reference point, McJannet et al. (2013a) found that using data from a weather station data located 3.4 km from the test lake led to an evaporation estimate that was 14 % larger than that based on shoreline measurements, but only 8 % larger than that based on overwater measurements. Finally, the method presented here used a range of coefficients and parameters that are typical of those reported in the literature. As such, they are generic values as opposed to site specific. Many of these parameters vary considerably in the literature, and, as such, the method would benefit from lake specific calibrated parameter sets.

Future research would enable further development of this method. For example, the application of the method described to a more instrumented lake could be used to investigate the impact of using remote data on the resulting evaporation measurements. Measuring the meteorological conditions on the lake shore or lake surface could be used to quantify the potential error associated with using remote weather station data. Likewise, local measurement of lake surface temperature could be used to assess the quality of the MODIS data. These measurements could also be used to validate the use of the HANTS algorithm for filling in missing MODIS data. Comparison with on-lake measurements of evaporation using, for example, an eddy co-variance probe or scintillometer would also better parameterize the remotely sensed evaporation measurements against more direct local measurements. In fact, given the availability of historical data going back to June 2002, this approach could be compared with previously published evaporation studies.

Acknowledgments The authors would like to thank the editor and reviewers for their time and constructive input. The revised paper is significantly improved as a result of their comments. Pan evaporation data for Clemson, SC were obtained from NOAA's National Climatic Data Center (NCDC). Ambient weather data were obtained from the National Weather Service Automated Surface Observing System (ASOS). Lake surface temperatures were obtained from the NASA Earth Observing System Data and Information System (EOSDIS). The authors thank Seann Reed of NOAA for his assistance in providing digitized evaporation atlas maps. This work was funded by the South Carolina Water Resources Center of Clemson University via the USGS whose support is gratefully acknowledged. This material is partially based on work supported by the National Science Foundation under Grant No. 1011478. Any opinions, findings, and conclusions or recommendations expressed in the material are those of the authors and do not necessarily reflect the views of the National Science Foundation.

Compliance with ethical standards

Conflicts of interest The authors declare that they have no conflict of interest. This article does not contain any studies with human participants or animals performed by any of the authors.

References

Adams EE, Cosler DJ, Helfrich KR (1990) Evaporation from heated water bodies: predicting combined forced plus free convection. Water Resour Res 26(3):425–435

Assouline S (1993) Estimation of lake hydrologic budget terms using the simultaneous solution of water, heat, and salt balances and a Kalman filtering approach: Application to Lake Kinneret. Water Resour Res 29(9):3041–3048

Assouline S, Mahrer Y (1993) Evaporation from Lake Kinneret: 1. Eddy correlation system measurements and energy budget estimates. Water Resour Res 29(4):901–910

Barnes GT (1968) Role of monolayers in evaporation retardation. Nature 220:1025–1026

Blanken PD, Rouse WR, Culf AD, Spence C, Boudreau LD, Jasper JN, Kochtubajda B, Schertzer WM, Marsh P, Verseghy D (2000) Eddy covariance measurements of evaporation from Great Slave Lake, Northwest Territories, Canada. Water Resour Res 36(4):1069–1077

Blanken PD, Rouse WR, Schertzer WM (2003) Enhancement of evaporation from a large northern lake by the entrainment of warm, dry air. J Hydrometeorol 4(4):680–693

Bower SM, Saylor JR (2013) Sherwood-Rayleigh parameterization for evaporation in the presence of surfactant monolayers. AIChE J 59:303–315

Boyd CE (1985) Pond evaporation. Trans Am Fish Soc 114(2):299–303

Brutsaert W (1975) A theory for local evaporation (or heat transfer) from rough and smooth surfaces at ground level. Water Resour Res 11(4):543–550

Brutsaert WH (1982) Evaporation into the atmosphere: theory, history, and applications. D. Reidel Publishing Company, Dordrecht

Crosman ET, Horel JD (2009) MODIS-derived surface temperature of the Great Salt Lake. Remote Sens Environ 113:73–81

Dalton J (1802) On the constitution of mixed gases, on the force of steam of vapour from water and other liquids in different temperatures, both in a Torricellia vacuum and in air; on evaporation; and on the expansion of gases by heat. Mem Lit Philos Soc Manch 5(2):536–602

Farnsworth RK, Thompson ES, Peck EL (1982) Evaporation atlas for the contiguous 48 United States. Technical report, Office of Hydrology—National Weather Service

Finch J, Calver A (2008) Methods for the quantification of evaporation from lakes, prepared for the World Meteorological Organization Commission of Hydrology CEH Wallingford, UK

Gianniou SK, Antonopoulos VZ (2007) Evaporation and energy budget in Lake Vegoritis, Greece. J Hydrol 345:212–223

Grim JA, Knievel JC, Crosman ET (2013) Techniques for using MODIS data to remotely sense lake water surface temperatures. J Atmos Ocean Technol 30:2434–2451

Gupta RS (2001) Hydrology and hydraulic systems. Waveland Press Inc, Long Grove

Ham J (1999) Measuring evaporation and seepage losses from lagoons used to contain animal waste. Trans ASAE 42(5):1303–1312

HDR Engineering, Inc. of the Carolinas (2014) Comprehensive environmental, engineering, and economic impact analysis report for revising the 1968 operating agreement for the Keowee-Toxaway project. Technical report, Duke Energy

Henderson-Sellers B (1986) Calculating the surface energy balance for lake and reservoir modeling: a review. Rev Geophys 43(3):625–649

Julien Y, Sobrino JA, Verhoef W (2006) Changes in land surface temperatures and NDVI values over Europe between 1982 and 1999. Remote Sens Environ 103(1):43–55

Kohler M, Parmele L (1967) Generalized estimates of free-water evaporation. Water Resour Res 3(4):997–1005

La Mer VK (ed) (1962) Retardation of evaporation by monolayers: transport processes. Academic Press, New York

Linsley R, Kohler M, Paulhus J (1982) Hydrology for engineers. McGraw-Hill Book Company, New York

Liu G, Ou W, Zhang Y, Wu T, Zhu G, Shi K, Qin B (2015) Validating and mapping surface water temperatures in Lake Taihu: results from MODIS land surface temperature products. IEEE J Sel Top Appl Earth Observ Remote Sens 8:1230–1244

Liu H, Blanken PD, Weidinger T, Nordbo A, Vesala T (2011) Variability in cold front activities modulating cool-season evaporation from a southern inland water in the USA. Environ Res Lett 6(2):024022

McGloin R, McGowan HA, Cook F, Sogachev A, Burn S (2014) Quantification of surface energy fluxes from a small body of water using scintillometry and eddy covariance. Water Resour Res 50:494–513

McJannet DL, Cook FJ, McGloin RP, McGowan HA, Burn S (2011) Estimation of evaporation and sensible heat flux from open water using a large-aperture scintillometer. Water Resour Res. doi:10.1029/2010WR010155

McJannet DL, Cook FJ, Burn S (2013a) Comparison of techniques for estimating evaporation from an irrigation water storage. Water Resour Res 49:1415–1428

McJannet D, Cook F, McGloin R, McGowan H, Burn S, Sherman B (2013b) Long-term energy flux measurements over an irrigation water storage using scintillometry. Agric For Meteorol 168:93–107

McMillan W (1971) Heat dispersal - lake Trawsfynydd cooling studies. Symposium on freshwater biology and electrical power generation, pp 41–80

Momii K, Ito Y (2008) Heat budget estimates for Lake Ikeda, japan. J Hydrol 361:362–370

Nadolski VL (1998) Automated surface observing system (ASOS) user's guide. S. Navy, Technical report, NOAA, DOD, FAA and U

Oesch DC, Jaquet J-M, Hauser A, Wunderle S (2005) Lake surface water temperature retrieval using advanced very high resolution radiometer and moderate resolution imaging spectroradiometer data: validation and feasibility study. JGR, 110

Patra K (2001) Hydrology and water resources engineering. Narosa Publishing House, Chennai

Penman HL (1948) Natural evaporation from open water, bare soil and grass. Proc R Soc Lond Ser A Math Phys Sci 193(1032):120–145

Reinart A, Reinhold M (2008) Mapping surface temperature in large lakes with MODIS data. Remote Sens Environ 112:603–611

Rimmer A, Samuels R, Lechinsky Y (2009) A comprehensive study across methods and time scales to estimate surface fluxes from Lake Kinneret, Israel. J Hydrol 379:181–192

Sartori E (2000) A critical review on equations employed for the calculation of the evaporation rate from free water surfaces. J Sol Energy 68:77–89

Saylor JR, Smith GB, Flack KA (2000) The effect of a surfactant monolayer on the temperature field of a water surface undergoing evaporation. Int J Heat Mass Trans 43:3073–3086

Schneider P, Hook SJ (2010) Space observations of inland water bodies show rapid surface warming since 1985. Geophys Res Lett 37(22):L22405

Stannard DI, Rosenberry DO (1991) A comparison of short-term measurements of lake evaporation using eddy correlation and energy budget methods. J Hydrol 122(1–4):15–22

Sweers H (1976) A nomogram to estimate the heat-exchange coefficient at the air-water interface as a function of wind speed and temperature; a critical survey of some literature. J Hydrol 30:375–401

US Army Corps of Engineers (2013) Savannah River Basin water management: frequently asked questions

US-EPA, Region 4, SESD (1999) Savannah River Basin REMAP: a demonstration of the usefulness of probability sampling for the purpose of estimating ecological condition in state monitoring programs. Technical report, Ecological Assessment Branch (EPA)

Verburg P, Antenucci JP (2010) Persistent unstable atmospheric boundary layer enhances sensible and latent heat loss in a tropical great lake: Lake Tanganyika. J Geophys Res 115(D11)

Wan Z (1999). MODIS land-surface temperature algorithm theoretical basis document (LST ATBD). Technical report, Institute for computational earth system science—University of California, Santa Barbara

Wan Z (2008) New refinements and validation of the MODIS land-surface temperature/emissivity products. Remote Sens Environ 112:59–74

Wan Z, Zhang Y, Zhang Q, Li Z-L (2002) Validation of the land-surface temperature products retrieved from Terra moderate imaging spectroradiometer data. Remote Sens Environ 83:163–180

Wan Z, Zhang Y, Zhang Q, Li Z-L (2004) Quality assessment and validation of the MODIS global land surface temperature. Int J Remote Sens 25:261–274

Webb EK, Pearman GI, Leuning R (1980) Correction of flux measurement of density effects due to heat and vapour transfer. Q J R Meteorol Soc 106:85–100

Winter TC, Buso DC, Rosenberry DO, Likens GE, Sturrock AM, Mau DP (2003) Evaporation determined by the energy-budget method for Mirror Lake, New Hampshire. Limnol Oceanogr 48(3):995–1009

Xiao F, Ling F, Du Y, Feng Q, Yan Y, Chen H (2013) Evaluation of spatial-temporal dynamics in surface water temperature of Qinghai Lake from 2001 to 2010 by using MODIS data. J Arid Land 5:452–464

Xu Y, Shen Y, Wu Z (2013) Spatial and temporal variations of land surface temperature over the Tibetan plateau based on harmonic analysis. Mt Res Dev 33(1):85–94

Yu SL, Brutsaert W (1967) Evaporation from very shallow pans. J Appl Meteorol 6:265–271